CHEMISTRY
A EUROPEAN JOURNAL

Prediction of Heterofullerene Stabilities: A Combined DFT and Chemometric Study of $C_{56}Pt_2$, $C_{57}Pt_2$ and $C_{81}Pt_2$

Josep M. Campanera,[a] Carles Bo,[a, b] Alan L. Balch,[c] Joan Ferré,[d] and Josep M. Poblet*[a]

Abstract: A systematic search of the regioisomers of the heterofullerenes, $C_{57}Pt_2$ and $C_{56}Pt_2$, has been carried out by means of density functional calculations to find the most stable structures. Both heterofullerenes incorporate two metal atoms into the fullerene surface. In the case of $C_{57}Pt_2$, one platinum atom substitutes one carbon atom of C_{60} and the other platinum atom replaces a C–C bond, whereas in $C_{56}Pt_2$ each platinum atom replaces one C–C bond. Several geometric factors were studied, three of which have particularly important effects on the relative stabilities of the regioisomers: the Pt–Pt separation, the number of C–C bonds remaining after substitution, and the type of C–C bond that is substituted. All these factors indicate that the deformation of the carbon framework is a general factor that governs the relative stabilities of the regioisomers. Because a high number of factors affect the stability of the heterofullerenes we also used chemometric techniques in this study. Partial least-squares (PLS) regression was used to establish the structure–energy relationships of $C_{57}Pt_2$ and $C_{56}Pt_2$ heterofullerenes. The understanding gained of the factors that affect the relative isomers stabilities has allowed us to predict the stabilities of larger disubstituted carbon cages, for example, $C_{81}Pt_2$ heterofullerene.

Keywords: chemometrics · density functional calculations · fullerenes · heterofullerenes · stability prediction

Introduction

Heterofullerenes are the third fundamental group of modified fullerenes, which also includes the more commonly studied exohedral and endohedral fullerene derivatives.[1] These heterofullerenes incorporate dopant atoms into the fullerene network by the replacement of certain carbon atoms with a variety of other atoms: nitrogen[2] and boron[3] incorporated into C_{60}, and arsenic,[4] phosphorus,[5] nitrogen[6] and boron[7] into the C_{70} framework. The development of heterofullerene isomerism has recently been described in a paper by Jiao et al. and references therein.[8] In recent years, several groups have identified fullerene clusters with metallic heteroatoms incorporated into the carbon framework. Branz and co-workers reported heterofullerenes with the compositions $C_{59-2n}M$ and $C_{69-n}M$, where M = Si, Fe, Co, Ni, Rh, and Ir and $n = 0$, 1, and 2.[9] Fullerenes with transition-metal atoms substituted into the carbon framework have also been observed in laser ablation studies:[10] $[C_{59}Pt]^+$, the result of replacing a carbon atom with a platinum atom, and $[C_{58}Pt]^-$, the result of the substitution of two carbon atoms by a platinum atom within a C_{60} molecule. In addition, the $[C_{57}Pt_2]^-$ and $[C_{56}Pt_2]^-$ ions, which incorporate two platinum atoms into the cage, have been detected.[10]

[a] J. M. Campanera, Dr. C. Bo, Prof. J. M. Poblet
Departament de Química Física i Inorgànica
Universitat Rovira i Virgili
Plaça Imperial Tàrraco 1, 43005 Tarragona, Catalonia (Spain)
E-mail: poblet@quimica.urv.es

[b] Dr. C. Bo
Institute of Chemical Research of Catalonia (ICIQ)
43007 Tarragona, Catalonia (Spain)

[c] Prof. A. L. Balch
Department of Chemistry, University of California
Davis, CA 95616 (USA)

[d] Dr. J. Ferré
Departament de Química Analítica i Química Orgànica
Universitat Rovira i Virgili
Plaça Imperial Tàrraco 1, 43005 Tarragona, Catalonia (Spain)

Supporting information for this article is available on the WWW under http://www.chemeurj.org/ or from the author. Description and numbering scheme for the regioisomers of $C_{57}Pt_2$ and $C_{56}Pt_2$ heterofullerenes, including symmetry, substituted C–C bonds and type of substituted C–C bonds. Substitution (SE) and binding energies (BE) for several heterofullerenes. Description of all different C–C bonds in the D_{2d}-(C_{84}:**23**) fullerene, including C–C bond lengths and pyramidalisation angle. Also additional graphs from the chemometric study are presented.

DOI: 10.1002/chem.200400814

Laser ablation of a $C_{60}/Ir(CO)_2$ film produces a number of products, $[C_{59}Ir]^-$, $[C_{58}Ir]^-$, $[C_{57}Ir]^-$, and $[C_{56}Ir]^-$, in which an iridium atom has replaced one or two carbon atoms within the fullerene cage. The ability of the metal atoms to bind added ligands has been demonstrated in laser ablation studies in the presence of 2-butene. In these cases, adducts such as $[C_{59}Ir(2\text{-butene})]^-$, $[C_{58}Ir(2\text{-butene})]^-$, $[C_{57}Ir(2\text{-butene})]^-$, and $[C_{56}Ir(2\text{-butene})]^-$ have been observed.[11]

As far as theory is concerned, semiempirical methods have been used to study the regioisomerism of nitrogen- and boron-doped fullerenes[12,13] and C_{60} doped with other atoms including oxygen, sulfur[14] and aluminium.[15] Density functional theory (DFT)-based calculations have been performed to study the structure and the electronic properties of $C_{59}M$ (M = Si,[16] Pt, Ir,[17] Fe, Co, Ni, and Rh[18]) and $C_{69}M$ (M = Co, Rh and Ir)[19] heterofullerenes. In $C_{59}M$, the metal atom is bonded to three carbon atoms; since the M–C bonds are longer than C–C bonds, the metal atoms protrude outward from the fullerene surface. The electronic structure of $C_{59}M$ varies with the metal and can be described in terms of the defect levels in the free fullerene host, C_{60}.[18] Computational studies performed on $C_{69}M$, where M = Co, Rh, and Ir, have shown that substitution at the more highly pyramidalized poles of the fullerene is energetically preferred.[19] In $C_{58}M$, the metal atom is linked to four carbon atoms and is positioned near the surface of the carbon cage. DFT calculations have proved that the isomer in which the metal atom replaces a C_2 unit at a [6:6] ring junction of the fullerene ($C_{58}M$:66) is significantly more stable than the isomer in which the metal replaces a C_2 unit at a [6:5] ring junction ($C_{58}M$:65).[11]

Abstract in Catalan: *En aquest treball portem a terme una cerca sistemàtica dels regioisòmers dels heteroful·lerens $C_{57}Pt_2$ i $C_{56}Pt_2$ amb l'objectiu de trobar les estructures més estables per cada estequiometria. Ambdós heteroful·lerens incorporen dos metalls a l'estructura del C_{60}. En el cas del $C_{57}Pt_2$ un Pt substitueix un carboni i l'altre un enllaç C–C, mentre que en el cas del $C_{56}Pt_2$, cadascun dels dos Pt substitueix un enllaç C–C. S'han estudiat diversos factors geomètrics, però només tres tenen efectes importants sobre l'estabilitat relativa dels regioisòmers: la separació Pt–Pt, el nombre d'enllaços C–C restants després de la substitució i el tipus d'enllaç C–C substituït. No obstant, tots els factors apunten que la deformació de l'estructura de la caixa carbònica governa l'estabilitat relativa dels regioisòmers. Degut al gran nombre de factors que poden intervenir en l'estabilitat s'usen tècniques d'anàlisi multivariant de dades. Així, la regressió per mínims quadrats parcials (PLS) facilità i sistematitzà la cerca de relacions entre l'estructura i l'estabilitat dels diferents regioisòmers pels heteroful·lerens $C_{56}Pt_2$ i $C_{57}Pt_2$. L'entesa dels factors que afecten l'estabilitat relativa d'aquests regioisòmers permeté la predicció de l'estabilitat de regioisòmers d'heteroful·lerens majors, com ara el $C_{81}Pt_2$.*

The substitution of two C_2 units or one C_2 unit and one carbon atom in C_{60} produces a very large number of regioisomers, which complicates the theoretical analysis of these dimetallic compounds. Herein, we report a detailed DFT study of the factors that govern the relative stabilities of the regioisomers of the $C_{56}Pt_2$ and $C_{57}Pt_2$ heterofullerenes. Based on these results, a multivariate regression model allowed a structure–energy relationship to be established. Furthermore, we used this information to develop a predictive model.

Computational Details

The calculations were carried out with the ADF2000 program using DFT methods.[20] The local density approximation (LDA), characterized by the electron-gas exchange, was used together with the Vosko–Wilk–Nusair[21] (VWN) parametrisation for correlation. Gradients were corrected by means of Becke[22] and Perdew[23] nonlocal corrections to the exchange and correlation energy, respectively. Triple-ζ and polarisation Slater basis sets were used to describe the valence electrons of the carbon and titanium atoms. A frozen core consisting of 1s and 1s,2p shells was described by means of single Slater functions for the carbon and titanium atoms, respectively. For platinum atoms, the inner electrons (from 1s to 4spd) were considered frozen and were described by means of single Slater functions, the 5s and 5p electrons by double-ζ Slater functions, 5d and 6s electrons by triple-ζ functions and 6p electrons by a single orbital.[24] The ZORA formalism with corrected core potentials was used to make quasirelativistic corrections to the core electrons. The quasirelativistic frozen core shells were generated with the auxiliary program DIRAC.[20] Open-shell electronic configurations were computed by using unrestricted methods. The Xaim program was used to investigate the topological properties of the electronic charge density between metal atoms.[25] Partial least-squares (PLS)[26] regression with full cross-validation was carried out by using the Unscrambler 8.0 software package.[26c]

Results

Regioisomers of $C_{57}Pt_2$: All the carbon atoms in C_{60} are equivalent. As a result, the $C_{59}Pt$ heterofullerene exists as a single isomer in which the metal center is tricoordinate. The $C_{57}Pt_2$ heterofullerene may be viewed as a derivative of $C_{59}Pt$ in which one of the C–C bonds has been substituted by a second platinum atom. There are 43 different regioisomers of $C_{57}Pt_2$. One of the platinum atoms in these regioisomers is tricoordinate, while the other is tetracoordinate. Owing to the high number of regioisomers it was necessary to select the isomers to be computed. Figure 1a shows the Schlegel diagram of C_{60} with the systematic numbering system recommended by IUPAC.[27] We considered first the series of regioisomers with C_s symmetry [$C_{57}Pt_2$:**1–7**]. In these regioisomers, one platinum atom replaces the C1 atom and the second platinum atom successively replaces the C25–C26, C44–C45, C57–C58, C52–C60, C35–C36, C16–C17, and C3–C4 bonds. These regioisomers are represented schematically by the Schlegel diagram in Figure 1b as follows: the first platinum atom is represented by a black dot and the position of the second by the position of the isomer number. All the regioisomers of $C_{57}Pt_2$ are also tabu-

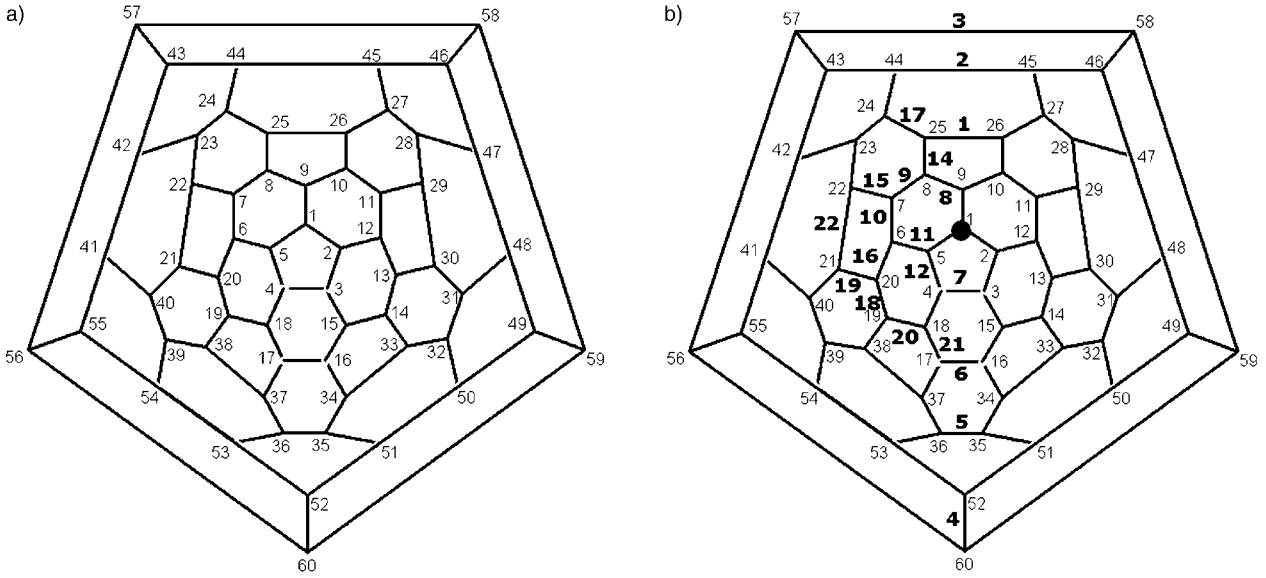

Figure 1. Schlegel diagrams showing the numbering system for a) C_{60} and b) the regioisomers of $C_{57}Pt_2$. The small numbers represent the numbering of C_{60}. The tricoordinate platinum atom is indicated by the black dot. The larger bold numbers represent the position of the tetracoordinate platinum atom and the regioisomer number. For instance, the regioisomer [$C_{57}Pt_2$:**1**] is constructed after the substitution of the C1 atom by the first metal atom and the substitution of the C25–C26 bond by the second metal atom.

lated in Table S1 of the Supporting Information together with the symmetry, the substituted C–C bond and the type of C–C bond. Figure 2 shows a plot of the computed relative energies of these regioisomers against the Pt–Pt separation in each isomer. The squares in Figure 2 represent the set of seven regioisomers with C_s symmetry; a dependence between the separation of the heteroatoms and the isomer stability is evident. Semiempirical studies on heterofullerenes $C_{60-n}X_n$ (X = N and B, n = 2–8)[12] and $C_{70-n}X_n$ (X = N and B, n = 2–10)[13] have also shown that the stabilities of the regioisomers decrease as the distance between the heteroatoms increases.

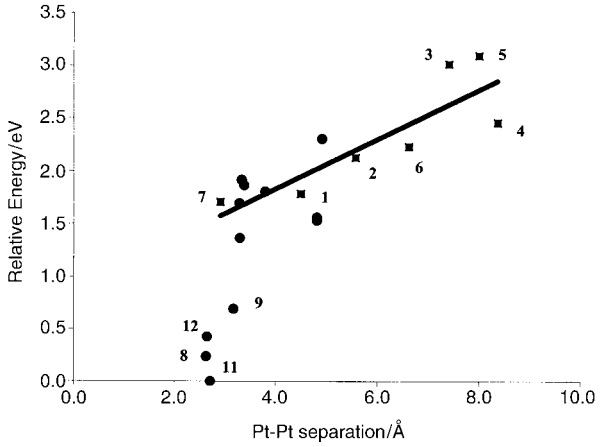

Figure 2. Relationship between Pt–Pt separation and the stability of the different regioisomers of $C_{57}Pt_2$. The first series of regioisomers, [$C_{57}Pt_2$:**1–7**], are represented by squared dots and the rest of the regioisomers, [$C_{57}Pt_2$:**8–22**], by circles. All the regioisomers of the first series are shown in the plot to determine the relationship between Pt–Pt separation and isomer stability. [$C_{57}Pt_2$:**11**] is the most stable regioisomer with a Pt–Pt distance of 2.708 Å and the least stable is [$C_{57}Pt_2$:**5**] with a distance of 7.998 Å between the two metal atoms. The linear correlation was performed by using the values for the regioisomers [$C_{57}Pt_2$:**1–7**]. The Pt–Pt separations and the relative energies of all the regioisomers of $C_{57}Pt_2$ are listed in Table 4.

In the second series of regioisomers, each of the C–C bonds in the hemisphere in which the first substitution occurs was replaced by a second platinum atom to give the regioisomers [$C_{57}Pt_2$:**8–22**] (see Figure 1b). These regioisomers have no symmetry elements. The assumption that substitution of sites neighbouring the original substituted atom yields stable structures is confirmed. The new regioisomers [$C_{57}Pt_2$:**8, 11**, and **12**] have the lowest relative energies. The most stable regioisomer corresponds to the substitution of the [6:6] C–C bond nearest to the previously substituted C1 atom (C6–C5), regioisomer [$C_{57}Pt_2$:**11**], whereas the next two regioisomers, [$C_{57}Pt_2$:**8** and **12**], correspond to the substitution of [6:5] C–C bonds nearest to the previously substituted C1 atom, C8–C9 and C4–C5, respectively. All the regioisomers of $C_{57}Pt_2$ are fully described in Table S1 in the Supporting Information. The correlation between Pt–Pt separation and the relative energies of the regioisomers shown in Figure 2 indicates that Pt–Pt separation is one of the main factors that govern the stability of the different regioisomers. However, there is no direct correlation between the two variables. The relatively short Pt–Pt distances in the three most stable regioisomers (2.708 Å for [$C_{57}Pt_2$:**11**], 2.626 Å for [$C_{57}Pt_2$:**8**] and 2.643 Å for [$C_{57}Pt_2$:**12**], see Figure 2) suggest the presence of some metal–metal interactions (see the section Metal–metal coupling below).

Figure 3 shows two views of the optimized structure of regioisomer [$C_{57}Pt_2$:**11**]. Like $C_{59}Pt$, the tricoordinate platinum

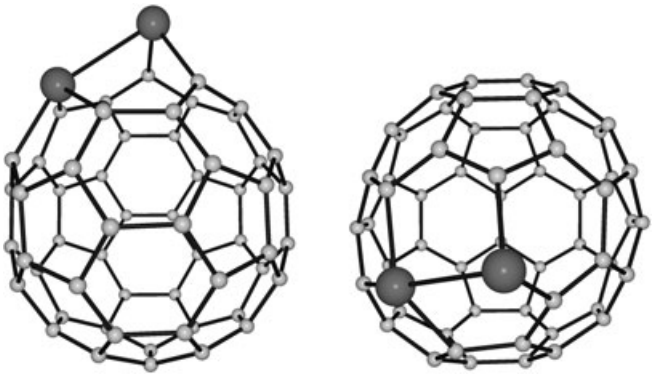

Figure 3. Different views of the optimized structure of the most stable regioisomer [$C_{57}Pt_2$:**11**].

atom with Pt–C bond lengths of 1.956 Å sticks out from the fullerene surface. The tetracoordinate platinum atom has a somewhat longer Pt–C distance (2.025 Å) and is located near the fullerene surface in the same way as in $C_{58}Pt$. Heteroatoms such as nitrogen or boron, which replace a single carbon atom, do not cause such a large deformation since the B–C and N–C bond lengths[15] (1.54 Å in $C_{59}B$ and 1.44 Å in $C_{59}N$) are more similar to the C–C bond lengths (1.398 Å for the [6:6] C–C bond and 1.453 Å for the [6:5] C–C bond) than are the Pt–C bond lengths. The position of the tricoordinate platinum atom in the $C_{57}Pt_2$ heterofullerene can be compared with the situation in $C_{59}M$ (M = Fe, Co, Ni, Rh, Ir and Pt). The large deformation of the carbon cage in regioisomer [$C_{57}Pt_2$:**11**] can be clearly seen in Figure 3.

Regioisomers of $C_{56}Pt_2$: We followed a similar strategy to construct the regioisomers of $C_{56}Pt_2$. When two C_2 units are substituted by two metal atoms the number of possible regioisomers is even larger than for the $C_{57}Pt_2$ heterofullerene. Consequently, we began by exploring the dependence of the isomer stability on the separation of the two tetracoordinate platinum atoms. The first nine regioisomers [$C_{56}Pt_2$:**1–9**] incorporate both platinum atoms into the main symmetry plane of C_{60}. These nine structures can be formally separated into two subsets: in the first, one platinum replaces the [6:6] C1–C9 bond and the second platinum atom successively replaces the C_2 units at C3–C4, C16–C17, C35–C36, and C52–C60 to produce regioisomers [$C_{56}Pt_2$:**1–4**]. In the second subset, the first heteroatom replaces the [6:5] C3–C4 bond and the second metal atom successively substitutes the C–C bonds in the symmetry plane (but not the previously substituted sites) to form regioisomers [$C_{56}Pt_2$:**5–9**]. A schematic representation of all these regioisomers is shown in Figure 4 and they are fully described in Table S2 in the Supporting Information. As in $C_{57}Pt_2$, there is no strict relationship between Pt–Pt separation and isomer stability, although in general the cluster is less stable when the two metal atoms occupy opposite hemispheres of the fullerene. Since the regioisomers are more stable when the two heteroatoms of the fullerene are in the same hemisphere, those regioisomers of $C_{56}Pt_2$ which have a Pt–Pt separation less than 5 Å were constructed and computed. With this restriction, 12 additional structures, regioisomers [$C_{56}Pt_2$:**10–21**], corresponding to substitutions of neighboring C_2 units were created, nine of which were nonsymmetric. The two most stable, [$C_{56}Pt_2$:**10** and **11**], are separated by only 0.037 eV. Figure 5

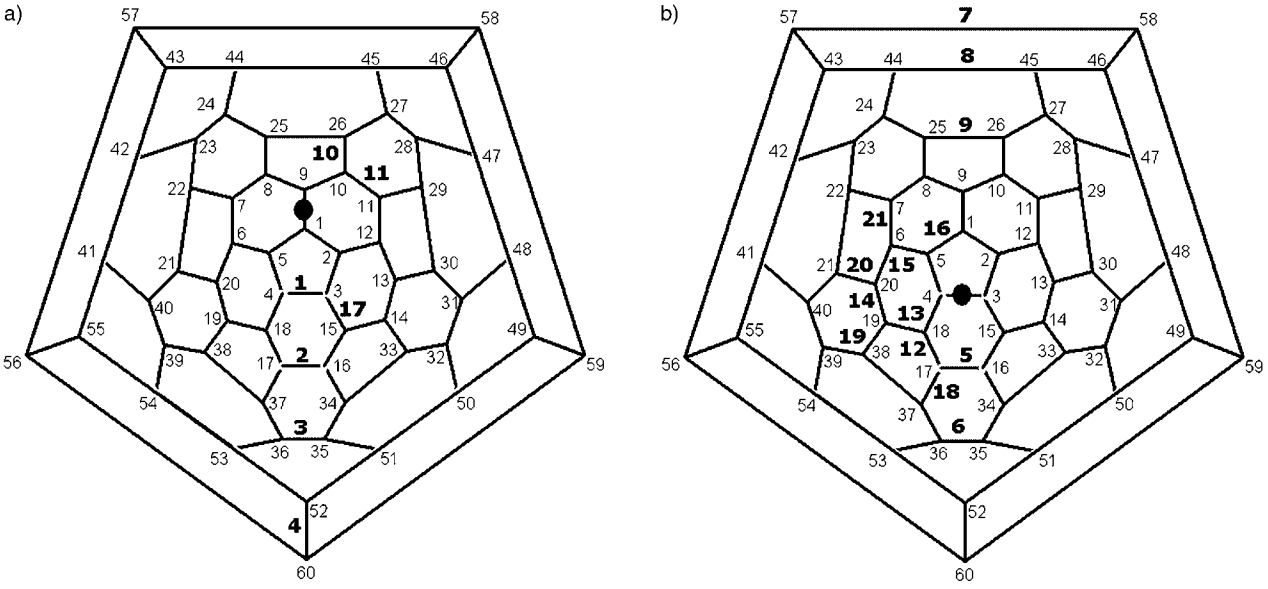

Figure 4. Schlegel diagrams showing the numbering system for regioisomers of $C_{56}Pt_2$. The small numbers represent the numbering of C_{60}. The first platinum atom is represented by the black dot. In a) the first platinum atom replaces the [6:6] C1–C9 bond whereas in b) the first platinum atom replaces the [6:5] C3–C4 bond. The larger bold numbers represent the position of the second metal atom, with respect to the first one, and also the regioisomer number. For instance, the regioisomer [$C_{57}Pt_2$:**10**] is constructed by substitution of the C1–C9 and C10–C26 bonds by two platinum atoms.

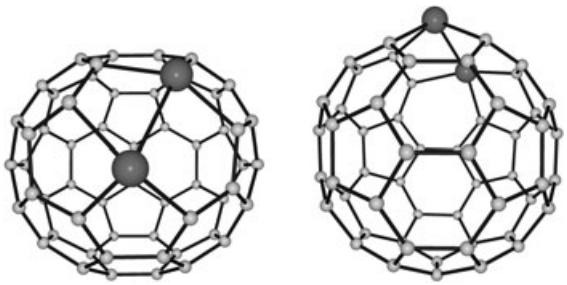

Figure 5. Different views of the optimized structure of the most stable regioisomer [$C_{56}Pt_2$:**10**].

shows the optimized structure of the most stable regioisomer, [$C_{56}Pt_2$:**10**].

Stability and electronic structure: At the level of theory used in this work, the binding energy (BE) per atom of C_{60} is −7.36 eV. In general, the substitution of a carbon atom in C_{60} by a metal atom is a highly endothermic process. The substitution energy (SE) for this process is computed to be 6.20 eV and the BE per atom of $C_{59}Pt$ is reduced to −7.25 eV. The SEs and BEs for mono- and diheterofullerenes are listed in Table S3 in the Supporting Information. The SE is corrected by using the energy of the true atomic ground state of the platinum and carbon atoms.[28] When the metal atom replaces a [6:6] C_2 bond to give $C_{58}Pt$ and C_2, the SE involved is 7.35 eV. A subsequent C_2 substitution in $C_{58}Pt$ to give the $C_{56}Pt_2$ diheterofullerene requires a similar amount of energy, more than 6 eV. The analogous process that converts $C_{59}Pt$ to $C_{57}Pt_2$ is less endothermic (4.88 eV). Hence, in the disubstituted cluster the BE per atom is reduced to −7.16 and −7.19 eV for $C_{56}Pt_2$ and $C_{57}Pt_2$, respectively. Semiempirical studies of boron and nitrogen heterofullerenes of C_{60}[12] and C_{70},[13] and DFT calculations on $C_{59}M$ (M = Fe, Co, Ni, and Rh),[18] also confirm that when the number of heteroatoms increases the stability is seriously affected.

The ground states of the two most stable regioisomers, [$C_{56}Pt_2$:**10** and **11**], are both singlets with relatively large HOMO–LUMO gaps of approximately 0.5 eV. As in $C_{59}Pt$ and $C_{58}Pt$, the highest occupied orbitals of regioisomers [$C_{56}Pt_2$:**10**] and [$C_{57}Pt_2$:**11**] are formally metal d orbitals. However, in the disubstituted heterofullerenes, the metal d orbitals are spread over several molecular orbitals. Specifically, in [$C_{56}Pt_2$:**10**] the contribution of the platinum d orbitals is 26% to the HOMO and 13% to the LUMO. In [$C_{57}Pt_2$:**11**], the metal contributions to the HOMO and LUMO are 15 and 12%, respectively. Ding et al.[18] described these metal-related orbitals in $C_{59}M$ heterofullerenes as defect levels in C_{60}. This means that heterofullerene orbitals can be seen as free C_{60} orbitals with a percentage contribution from the metal atoms and, as a result, the electronic structure depends on the incorporated metal atom. Nevertheless, it is interesting to note that the C-HOMO (the highest carbon-derived occupied orbital)–C-LUMO (the lowest carbon-derived unoccupied orbital) gap changes very little from one cluster to another and is very close to 1.65 eV, the gap of pure C_{60}. Similar behavior was observed for all the regioisomers of these diheterofullerenes since the C-HOMO–C-LUMO gap appears to be constant at ~1.6 eV.

Physical properties: Table 1 lists the ionisation potentials (IPs) and the electron affinities (EAs) of C_{60}, $C_{59}Pt$, $C_{58}Pt$, [$C_{56}Pt_2$:**10**], and [$C_{57}Pt_2$:**11**] together with the corresponding HOMO and LUMO energies. The computed IP and EA of free C_{60} (7.56 eV and 2.89 eV, respectively) are in good agreement with the experimental values (7.6 eV[29] and 2.7 eV[30]). In general, the incorporation of metal atoms into the carbon cage results in a reduction in the IP and EA of the cluster. For regioisomers [$C_{56}Pt_2$:**10**] and [$C_{57}Pt_2$:**11**], the computed IPs are 7.04 and 6.78 eV, respectively, and the corresponding EA values are 3.64 and 3.44 eV. Therefore, doping with platinum atoms enhances the redox properties of C_{60}. This observation has already been described for the monosubstituted clusters $C_{58}Pt$ and $C_{59}Pt$. However, the incorporation of new metal atoms into the fullerene skeleton of the monoheterofullerenes has little effect on the physical properties of the cluster. The same behavior was reported for $C_{60-n}N_n$ and $C_{60-n}B_n$ heterofullerenes.[12]

Table 1. Computed ionisation potentials (IP), electron affinities (EA) and HOMO and LUMO energies [all in eV] for several optimized heterofullerenes.

Molecule	Symmetry	IP	EA	*E*(HOMO)	*E*(LUMO)	HOMO–LUMO gap
C_{60}	I_h	7.56	2.89	−6.25	−4.59	1.66
$C_{58}Pt$:66	C_{2v}	7.37	3.67	−5.91	−5.37	0.54
$C_{59}Pt$	C_s	6.68	3.05	−5.38	−4.68	0.70
[$C_{56}Pt_2$:**10**]	C_1	7.04	3.64	−5.69	−5.20	0.49
[$C_{57}Pt_2$:**11**]	C_1	6.78	3.44	−5.53	−5.03	0.50

Metal–metal coupling: The short metal–metal distances found in the most stable regioisomers of $C_{57}Pt_2$ and $C_{56}Pt_2$ heterofullerenes suggest that significant metal–metal coupling occurs. Pt–Pt bond lengths smaller than 2.6 Å usually occur in platinum complexes in which the metal atoms are in low oxidation states. The mean Pt–Pt distance in the 53 examples held in the Cambridge Structural Database (CSD)[31] in which the platinum atom is tetracoordinate or tricoordinate with a 0 oxidation state is 2.643 ± 0.045 Å, and the shortest distance is 2.554 Å, which is found in the [Pt_2(μ-$OPPh_2$)($PMePh_2$)$_2$] complex (Refcode JEMLOC[32]). The Pt–Pt distances of the regioisomers considered here span a wide range, from 2.626 to 8.358 Å in $C_{57}Pt_2$ and from 2.683 to 7.750 Å in the $C_{56}Pt_2$ heterofullerene. Pt–Pt coupling has been investigated only in regioisomers with metal–metal distances shorter than 3 Å. Molecular orbital (MO) analysis does not allow conclusions about the nature of the metal–

metal interaction to be drawn because the d orbitals of platinum are spread across multiple MOs. The topological analysis of the total charge density function has proved to be a powerful tool in determining the bonding character of several kinds of bonds.[33,34] Our experience with transition-metal compounds shows that the lack of a bond critical point (bcp) linking two transition-metal atoms does not exclude the existence of metal–metal interactions. For example, a bcp was not detected between the titanium atoms in Ti_8C_{12} although there is a clear metal–metal interaction.[35] On the other hand, the presence of a bcp between two transition-metal atoms is strong evidence for coupling. The bonding and charge properties of these regioisomers and some others are given in Table 2.

Table 2. Parameters for determining the bonding character of the platinum–platinum bond.

Isomer number	Pt–Pt[a] [Å]	Bond critical point	No. of Pt–C bonds[b]	Sum of net Mulliken charges for both Pt atoms [*e*]
$C_{57}Pt_2$				
8	2.626	(3,−1)	2,3	1.168
12	2.643	(3,−1)	2,3	1.132
11	2.708	(3,−1)	2,3	1.189
7	2.905	(3,1)	3,4	1.608
9	3.171	(3,1)	3,4	1.564
3	7.408	–	3,4	1.588
$C_{56}Pt_2$				
1	2.683	(3,1)	4,4	1.583
16	2.683	[c]	3,3	1.301
5	2.700	(3,1)	4,4	1.583
13	2.714	(3,−1)	3,3	1.240
10	2.739	(3,−1)	3,3	1.249
11	2.836	(3,−1)	3,3	1.162
12	2.847	(3,−1)	3,3	1.124
18	2.856	(3,1)	4,4	1.514
14	2.863	(3,1)	4,4	1.469
15	2.866	(3,1)	4,4	1.526
3	7.071	–	4,4	1.654

[a] Pt–Pt separation. [b] Number of Pt–C bonds with a distance shorter than 2.212 Å. In the regioisomers of $C_{57}Pt_2$, the first number refers to the tricoordinate platinum atom and the second number to the tetracoordinate atom. In the regioisomers of $C_{56}Pt_2$, both platinum atoms are tetracoordinate. [c] No critical point was localized in regioisomer [$C_{56}Pt_2$:**16**], but a (3,−1) bcp is expected.

In $C_{57}Pt_2$, the platinum atoms in the three regioisomers with the shortest Pt–Pt separation, [$C_{57}Pt_2$:**8**, **11** and **12**] (see Table 2), were linked by bcps. In these clusters, the presence of a bcp coincides with platinum atoms with low coordination numbers. As seen in Figure 6, one of the metal atoms is coordinated to three carbon atoms and the other to two carbon atoms (coordination 3,2 in Figure 6). In all the other regioisomers, the platinum atoms are coordinated to four and three carbon atoms (coordination 4,3) and the result is a lack of any metal–metal interaction. The presence of a (3,+1) cycle critical point in the region between the two metal atoms in [$C_{57}Pt_2$:**7**], a cluster with a relatively short Pt–Pt distance of 2.905 Å, denotes the presence of direct metal–metal interactions. Mulliken net charges can also provide some clues about the metal–metal coupling. According to the sum of the net charges on both metals, there are two groups of heteroatoms: one group has a positive charge of approximately $+1.2e$ and corresponds to the metal atoms for which a bcp was characterized. The metal atoms in the other isomers have somewhat larger net charges, between $+1.5e$ and $+1.6e$. The low depopulation of the platinum orbitals in regioisomers [$C_{57}Pt_2$:**8**, **11** and **12**] permits a concentration of electron density in the intermetallic region, and this also indicates that metal–metal interactions occur in these clusters.

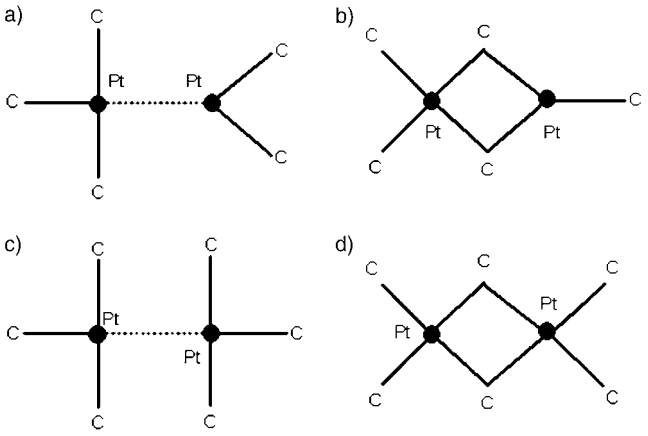

Figure 6. Schematic representation of the coordination of platinum atoms in the regioisomers of $C_{57}Pt_2$ and $C_{56}Pt_2$ in which the platinum–platinum distance is less than 3 Å. a) One platinum atom surrounded by three carbon atoms and the other by two (3,2 coordination), corresponding to regioisomers [$C_{57}Pt_2$:**8**, **11**, and **12**], b) 4,3 coordination corresponding to regioisomers [$C_{57}Pt_2$:**7** and **9**], c) 3,3 coordination corresponding to regioisomers [$C_{56}Pt_2$:**10**–**13**] and d) 4,4 coordination corresponding to regioisomers [$C_{56}Pt_2$:**1**, **5**, **14**, **15** and **18**].

The situation in $C_{56}Pt_2$ is not so simple. $C_{56}Pt_2$ has 10 regioisomers that have a Pt–Pt distance of less than 3 Å. In five of them, [$C_{56}Pt_2$:**10**–**13** and **16**], both of the platinum atoms are surrounded by three carbon atoms (coordination 3,3 in Figure 6), whereas in the other structures the metal is coordinated to four carbon atoms (coordination 4,4). The presence of a direct Pt–Pt interaction is only expected in the structures that have a 3,3 coordination. Indeed, bcp are only characterized for isomers with this low coordination, [$C_{56}Pt_2$:**10, 11, 12** and **13**] (Table 2). In all these structures, the trends in the Mulliken charges are the same as those observed for $C_{57}Pt_2$.

Discussion

Topological and structural factors that govern isomer stability: The substitution of several carbon atoms in a fullerene results in a high number of possible regioisomers and computation of all of these becomes unrealistic as the size of the fullerene increases. Therefore, it is necessary to know which factors determine the isomer stability and to have some information about how to carry out a search for the most

Table 3. Geometric factors affecting the stabilities of regioisomers of $C_{57}Pt_2$.

Isomer number	Relative energy	Topological factors				Structural factors				HOMA[a]
		Pt–Pt	no. C–C bonds	C–C bond type	no. hetero-rings	cage radius	Pt–C	[6:6] C–C	[6:5] C–C	
C_{60}		–	90	–	–	3.551	–	1.398	1.453	0.274
$C_{59}Pt$		–	87	–	3	3.580	1.982	1.400	1.452	0.268
$C_{58}Pt$	0.000	–	85	[6:6]	4	3.562	2.034	1.403	1.451	0.279
	0.630	–	85	[6:5]	4	3.569	2.031	1.400	1.453	0.240
11	0.000	2.708	83	[6:6]	5	3.587	1.997	1.400	1.451	0.279
8	0.237	2.626	83	[6:5]	5	3.592	1.999	1.400	1.452	0.263
12	0.426	2.643	83	[6:5]	5	3.592	2.007	1.399	1.452	0.259
9	0.692	3.171	82	[6:6]	6	3.591	2.028	1.400	1.451	0.285
13	1.368	3.289	82	[6:6]	7	3.598	2.030	1.403	1.451	0.313
17	1.531	4.806	82	[6:6]	7	3.593	2.025	1.401	1.450	0.287
18	1.562	4.809	82	[6:6]	7	3.590	2.020	1.403	1.450	0.304
10	1.696	3.280	82	[6:5]	6	3.595	2.020	1.399	1.452	0.265
7	1.708	2.905	82	[6:5]	7	3.595	2.005	1.401	1.452	0.237
1	1.787	4.493	82	[6:5]	7	3.596	2.024	1.399	1.452	0.263
15	1.808	3.792	82	[6:5]	6	3.606	2.034	1.398	1.452	0.271
14	1.866	3.376	82	[6:5]	6	3.602	2.024	1.401	1.451	0.283
16	1.917	3.327	82	[6:5]	6	3.605	2.022	1.402	1.451	0.276
2	2.126	5.566	82	[6:6]	7	3.590	2.012	1.405	1.450	0.276
6	2.230	6.614	82	[6:6]	7	3.590	2.012	1.404	1.449	0.284
4	2.456	8.358	82	[6:6]	7	3.591	2.011	1.405	1.451	0.273
19	2.303	4.903	82	[6:5]	7	3.598	2.021	1.399	1.450	0.269
21	2.624	4.837	82	[6:5]	7	3.599	2.019	1.404	1.451	0.271
20	2.765	4.762	82	[6:5]	7	3.598	2.015	1.401	1.452	0.257
22	2.912	5.193	82	[6:5]	7	3.600	2.010	1.403	1.452	0.241
3	3.014	7.408	82	[6:5]	7	3.599	2.012	1.402	1.452	0.238
5	3.094	7.998	82	[6:5]	7	3.599	2.012	1.402	1.452	0.243

[a] Taking into account only C–C bonds. For these bonds, HOMA was calculated with $\alpha = 257.7$ and $R_{opt} = 1.388$ according to reference [43].

stable structures in any substituted fullerene. Kurita and coworkers[36] have already pointed out that the electronic properties of $C_{58}X_2$ (X = B and N) largely depend on the relative positions of the heteroatoms in the heterofullerenes. Furthermore, Chen et al. have presented a systematic search in which the most stable isomer of $C_{58}X_2$ was found by using semiempirical methods.[37] If we know a priori where to look for the most stable structures of heterofullerenes, we will be able to save a huge amount of the computational effort involved in predicting electronic properties.

The most important factors that affect the stability of $C_{57}Pt_2$ and $C_{56}Pt_2$ are listed in Table 3 and Table 4, respectively. We classified these as topological and structural factors. The topological factors are those which provide constitutive information about each regioisomer and can be determined or estimated a priori without any calculation: the Pt–Pt separation,[38] the number of C–C bonds,[39] the type of substituted C–C bond[40] and the number of heterorings.[41] The structural factors characterise the geometry of each regioisomer in detail and can be determined once the geometry of the molecules is fully known. The structural factors considered here are the cage radius,[42] average bond lengths (Pt–C, [6:6] C–C and [6:5] C–C) and one geometric parameter of aromaticity, the harmonic oscillator model of aromaticity (HOMA).[43,44,45]

Structure–energy relationship: In fact, none of the nine factors by itself can satisfactorily explain the order of the relative energy or the groups of regioisomers observed according to their structure–energy relationship. Hence we decided to investigate the simultaneous (multivariate) relationship of the nine factors and the relative energy by using partial least-squares (PLS) regression analysis. This multivariate data analysis technique, which has become very popular in chemometrics in recent years,[46] can be used to search for combinations of the topological/structural factors (x variables) that best explain the relative energy (y variable). Each combination is called a latent variable (LV). The first latent variable (LV1) describes the largest part of the x variables that have the highest correlation with the relative energy. The second latent variable (LV2) describes the largest part of the variability left over by LV1, and so on. Hence, by considering only the first few latent variables we can study trends between the nine original factors/x variables and the relative energy without being blurred by the redundancy of the data.

An exploratory analysis using PLS regression was first applied to the data in Table 3.[47] Figure 7 shows the two-dimensional biplot (LV1 versus LV2) for the regioisomers of $C_{57}Pt_2$. The plot shows 60% of the original x data which are correlated to 95% of the y data. This means that 40% of

Table 4. Geometric factors affecting the stabilities of regioisomers of $C_{56}Pt_2$.

Isomer number	Relative energy	Topological factors					Structural factors			
		Pt–Pt	no. C–C bonds	C–C bond type	no. hetero-rings	cage radius	Pt–C	[6:6] C–C	[6:5] C–C	HOMA[a]
10	0.000	2.739	81	[6:6]/[6:5]	4	3.575	2.042	1.401	1.451	0.287
11	0.037	2.836	81	[6:6]/[6:6]	4	3.568	2.046	1.401	1.450	0.310
13	0.200	2.714	81	[6:5]/[6:5]	4	3.583	2.041	1.400	1.452	0.278
16	0.789	2.683	81	[6:5]/[6:5]	4	3.573	2.010	1.399	1.453	0.230
12	1.083	2.847	81	[6:5]/[6:5]	4	3.581	2.032	1.400	1.452	0.288
5	0.123	2.700	80	[6:6]/[6:5]	6	3.573	2.042	1.403	1.451	0.296
1	0.911	2.683	80	[6:6]/[6:5]	6	3.578	2.058	1.402	1.451	0.298
2	0.943	5.488	80	[6:6]/[6:6]	8	3.571	2.038	1.405	1.449	0.310
17	1.048	3.429	80	[6:6]/[6:6]	6	3.582	2.054	1.403	1.449	0.304
14	1.123	2.863	80	[6:5]/[6:6]	6	3.582	2.074	1.399	1.449	0.318
4	1.267	7.750	80	[6:6]/[6:6]	8	3.575	2.038	1.408	1.451	0.281
15	1.584	2.866	80	[6:5]/[6:5]	6	3.587	2.066	1.400	1.451	0.300
18	1.589	2.856	80	[6:5]/[6:5]	6	3.587	2.068	1.400	1.451	0.294
3	1.776	7.071	80	[6:6]/[6:5]	8	3.581	2.036	1.406	1.453	0.247
8	1.887	7.290	80	[6:5]/[6:6]	8	3.581	2.036	1.405	1.452	0.241
6	2.152	5.395	80	[6:5]/[6:5]	8	3.582	2.038	1.401	1.452	0.238
19	2.156	3.667	80	[6:5]/[6:5]	6	3.594	2.051	1.401	1.452	0.243
21	2.271	3.664	80	[6:5]/[6:5]	6	3.579	2.050	1.401	1.453	0.231
9	2.399	5.959	80	[6:5]/[6:5]	8	3.584	2.034	1.401	1.453	0.214
7	2.481	7.729	80	[6:5]/[6:5]	8	3.590	2.033	1.402	1.454	0.205
20	2.723	4.135	80	[6:5]/[6:5]	6	3.598	2.059	1.400	1.451	0.268

[a] Taking into account only C–C bonds. For these bonds, HOMA was calculated with $\alpha = 257.7$ and $R_{opt} = 1.388$ according to reference [43].

the x data is not relevant for describing the relative energy. Each regioisomer is indicated by a dot. Its position depends on the values of the x variables. Two regioisomers are close to each other when the values of their original x variables are similar. Their separation is large when the values of their x variables are very different. Each x variable is indicated by an arrow, which points in the direction of increasing values of that variable.

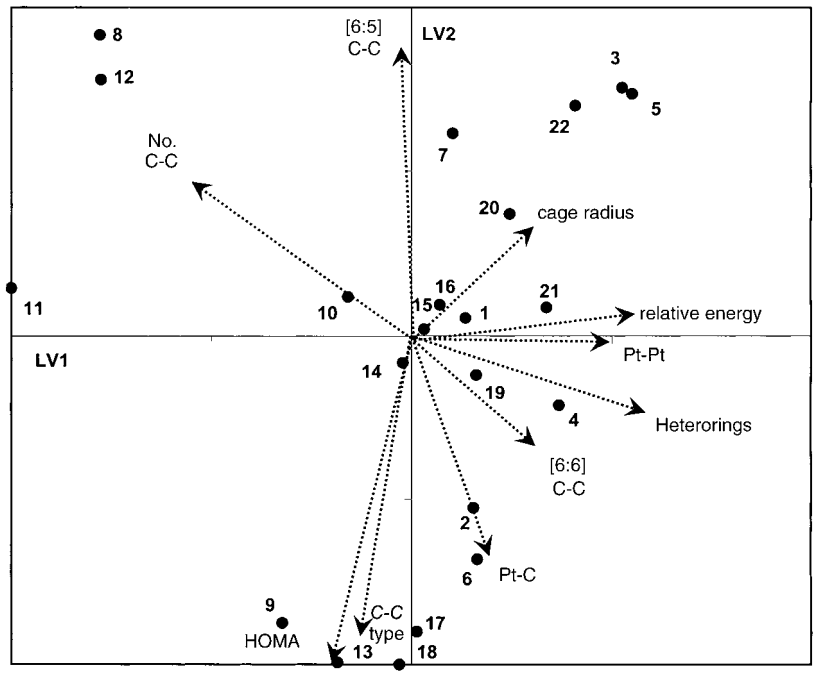

Figure 7. Biplot for the regioisomers of $C_{57}Pt_2$ obtained after PLS regression on the nine factors affecting the stability of the regioisomers. Dots represent regioisomers and arrows represent factors. The plot shows 60% of the x data, which are correlated to 95% of the y data.

By considering the regioisomers and original variables together, we can visually find similarities and differences between the regioisomers and study what variables are responsible for such interdependencies, thus obtaining chemical/structural information. The relative-energy arrow points in the direction of LV1 positive values (abscissa axis). Hence, LV1 can be used to determine the stabilities of the regioisomers, which decrease from left to right: [$C_{57}Pt_2$:**8**, **11** and **12**], on the far left, are the most stable and [$C_{57}Pt_2$:**3, 5** and **22**], on the far right, are the least stable. By considering the arrows of

the *x* variables that are most parallel to LV1, we note that the stability is mainly characterized by the combined effect of a short Pt–Pt separation, a small number of heterorings and a large number of retained C–C bonds. Regioisomers [$C_{57}Pt_2$:**8**, **11**, and **12**] have 83 C–C bonds, five heterorings and the shortest Pt–Pt separation. The regioisomers with fewer C–C bonds, a longer Pt–Pt separation and more heterorings are on the right. The other six variables contribute to the stability to a smaller extent. HOMA, C–C bond type and [6:5] C–C bond lengths are responsible for the position of the regioisomers at the top and bottom of the plot. As we move down-left, the regioisomers have higher HOMA values and [6:6] C–C substitution and a low [6:5] C–C distance. The combined effect of these three factors also makes the regioisomers more stable. For example, regioisomer [$C_{57}Pt_2$:**11**] is down-left relative to regioisomers [$C_{57}Pt_2$:**8** and **12**], which have smaller HOMA values, less [6:5] C–C bond substitution and larger [6:5] C–C distances. The same trend can also be observed with regioisomers [$C_{57}Pt_2$:**9**, **13**, **17**, and **18**] relative to [$C_{57}Pt_2$:**1**, **7**, **10**, **14**, **15**, and **16**], and regioisomers [$C_{57}Pt_2$:**2**, **4** and **6**] relative to [$C_{57}Pt_2$:**3**, **5**, **19**, **20**, **21**, and **22**]. An important conclusion can be drawn form this which will be studied later: the removal of [6:6] C–C bonds has less effect on the aromaticity of the cage than the removal of [6:5] C–C bonds. As far the cage radius, Pt–C distance and [6:6] C–C bond lengths are concerned, high values increase the instability of the regioisomers. This is to be expected for the cage radius since a high value indicates greater distortion.

The regression coefficients of the PLS model (Table 5) give a quantitative measure of the relative importance of each *x* variable in defining the stability of the regioisomers.

Table 5. Regression coefficients of the PLS model considering two latent variables.

Factor		$C_{57}Pt_2$	$C_{56}Pt_2$
topological	Pt–Pt	0.258	0.150
	no. C–C bonds	−0.218	−0.247
	C–C bond type	−0.134	−0.183
	no. heterorings	0.258	0.201
astructural	cage radius	0.179	0.307
	Pt–C	0.024	0.106
	[6:6] C–C	0.152	−0.055
	[6:5] C–C	0.023	0.104
	HOMA	−0.159	−0.200

A positive sign indicates that an increase in the value of the *x* variable increases the relative energy. A negative sign indicates the opposite effect. The sign agrees with the trends observed in the biplot. Based on the magnitude of these coefficients we can distinguish three groups. The largest regression coefficients correspond to those of the topological factors: Pt–Pt separation, the number of heterorings and the number of retained C–C bonds. The Pt–C and [6:5] C–C bond lengths are the two least important factors and the rest of the factors have an intermediate impact on the relative stability decreasing in the order: cage radius > HOMA > [6:6] C–C bond lengths. This result is quite significant since it suggests that the topological factors by themselves can provide an estimate of the relative energies of the regioisomers of $C_{57}Pt_2$. In fact we can judge the ability of the PLS model to predict the relative energy from the average error of the predictions. This value is given by the root-mean-squared error of prediction (RMSEP) calculated by cross-validation.[46] The model calculated with the nine *x* variables has a RMSEP of 0.233 eV, whereas the model calculated by considering only the four topological factors has a RMSEP of 0.288 eV. This result suggests that consideration of the remaining factors only slightly improves the prediction. In both cases, an average error of 0.233 or 0.288 eV is low enough relative to the range of relative energies (0–3.094 eV) to enable trends to be observed just from the predictions made using the geometric parameters of the molecule. A visual inspection of the quality of the prediction is shown in the plot of DFT-calculated relative energies versus PLS-predicted relative energies given in the Supporting Information (Figure S1).

The PLS analysis was also applied to the data for $C_{56}Pt_2$ in Table 4.[48] The trends observed in the structure–energy relationship are similar to those seen for the regioisomers of $C_{57}Pt_2$ although the difference between topological and structural factors is not so marked and the prediction of the relative stabilities for the regioisomers of $C_{56}Pt_2$ is less accurate (the PLS model of two latent variables yields a RMSEP of 0.379 eV). The numbers of C–C bonds and heterorings still have a significant impact on the relative energy but, in this case, the Pt–Pt distance has less impact on the stability while the cage radius and HOMA have a strong correlation with the stability of the heterofullerenes, see Table 5. We also realize that the Pt–C, [6:6] C–C and [6:5] C–C bond lengths have an ambiguous and weak correlation with the stability of the heterofullerenes and thus these factors are not important for describing the stability of heterofullerenes. This trend was also found in the analysis of $C_{57}Pt_2$.

Stability of the carbon skeleton is the principal factor that determines isomer stability: Without a doubt, the PLS technique has enabled us to determine structure–energy relationships and it has proved to be valid for analysing multivariate data. Apart from the stabilisation produced by the weak metal coupling detected in some regioisomers, the factors that dominate the structure–energy relationship are practically independent of the metal. In fact, the relative energy seems to be a measure of the distortion of the cage skeleton from the free equilibrium geometry produced by the inclusion of the two metal atoms. So the Pt–Pt separation, the number of C–C bonds, the type of substituted C–C bond, the number of heterorings, cage radius, the different bond lengths and the HOMA index are closely related and interdependent simply because they are all indirect measurements of this distortion. To confirm that the relative energies of the various regioisomers are independent of the incorporated metal atom, first we changed the number of electrons in several of the regioisomers of $C_{56}Pt_2$, performing

calculations on the cationic, $[C_{56}Pt_2]^+$, and anionic, $[C_{56}Pt_2]^-$ species (see Table 6). The regioisomers selected for the test are some of the most symmetric regioisomers from the

Table 6. Relative energies for different clusters.

Isomer number	Relative energy [eV]				
	$C_{56}Pt_2$	$[C_{56}Pt_2]^+$	$[C_{56}Pt_2]^-$	$C_{56}Ti_2$	C_{56}
10	0.00	0.00	0.00	0.00	0.00
11	0.04	−0.09	0.15	0.57	−1.06
2	0.94	1.07	0.75	1.06	2.27
4	1.27	1.27	1.04	1.40	2.58
6	2.15	2.27	2.17	2.35	4.07
9	2.40	2.38	2.57	2.58	4.14
7	2.48	2.59	2.58	3.08	4.25

groups with high, [$C_{56}Pt_2$:**10** and **11**], intermediate, [$C_{56}Pt_2$: **2** and **4**], and low, [$C_{56}Pt_2$:**6, 7**, and **9**], stability. In the cations, the positive charge is basically localized in both platinum atoms rather than in the carbon framework: for instance, the sum of the Mulliken net charge on both platinum atoms in [$C_{56}Pt_2$:**10**] was computed to be 1.249*e* and 1.333*e* in the corresponding cation. Despite the repulsion between the charges, the relative stabilities of the various regioisomers does not change (see Table 6). In the anion, all the additional charge is spread over the carbon framework and the relative energies of the regioisomers follows the same trend as shown by the neutral platinum analogue. Second, the incorporation of a different metal atom such as titanium was also tested; the order of the relative energy of the regioisomers was unchanged but their relative energies were higher. A titanium atom behaves like a platinum atom in the $C_{56}Pt_2$ heterofullerene because the computed Ti–C bond length is very similar to the Pt–C bond length in $C_{56}M_2$ heterofullerenes (2.098 Å versus 2.042 Å for [$C_{56}M_2$:**10**]). Finally, single point calculations were carried out by extracting platinum atoms from the optimized $C_{56}Pt_2$ structures. In this case we analyze the effect of a hole on the stability of the rest of the carbon skeleton. Determination of the electronic state of fullerenes with holes is not easy because of the presence of dangling bonds. The lowest electronic state of holed C_{58} fullerene formed from C_{60} by removal of a [6:6] C–C bond is a triplet but when two C_2 units are removed to form C_{56} the singlet competes with the triplet for the most stable electronic state, which is governed by the type of hole produced in C_{60}. As can be seen in Table 6, the order of the relative energies of the regioisomers follows the same trend as that shown by the regioisomers of $C_{56}Pt_2$, which confirms the general idea that the most important factor that governs the relative energies is the destabilisation of the carbon cage produced by the incorporation of a metal atom into the free carbon framework.

Prediction of the isomer stability of the $C_{81}Pt_2$ heterofullerene, a doped fullerene from the D_{2d}-(C_{84}:23) fullerene: In the previous sections, we have combined quantum chemistry (DFT) and chemometrics (PLS regression) to analyse and understand the stabilities of the computed regioisomers of $C_{57}Pt_2$ and $C_{56}Pt_2$. The low prediction error of 0.288 eV obtained for the PLS model of $C_{57}Pt_2$ calculated by using only topological factors encouraged us to go further. Since the four topological factors can be estimated a priori, we used PLS regression analysis to predict the trends in the stability of noncomputed structures of the same heterofullerenes or of larger clusters.

In larger fullerenes the complexity may be enormous. Consider for example C_{84}. This fullerene has 24 IPR isomers of which isomer **23** with D_{2d} symmetry has one of the lowest energies, similar to that of isomer **22** with D_2 symmetry.[49] In this section, we will show that we can use data from the heterofullerenes of C_{60} to determine the relative stabilities of other carbon cages. In particular, we have analysed the substitution of a C_2 unit and a carbon atom in the D_{2d}-(C_{84}:**23**) isomer.[50] The resulting $C_{81}Pt_2$ heterofullerene contains a tetracoordinate and tricoordinate platinum atom which is similar to the situation in $C_{57}Pt_2$. Pyramidalisation angles[51,52] and bond lengths of all the different C–C bonds

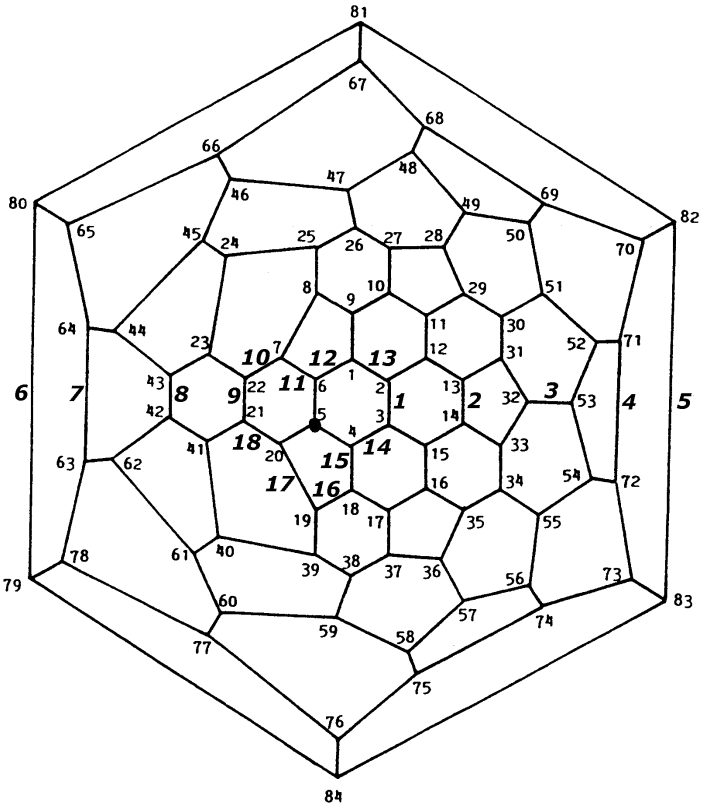

Figure 8. Schlegel diagram showing the numbering system for D_{2d} [C_{84}:**23**] fullerene (from ref. [50]) and regioisomers of $C_{81}Pt_2$. The small numbers represent the numbering of C_{84}. The tricoordinate heteroatom, which substitutes the C5 atom, is situated at the black dot. The larger bold numbers represent the position of the tetracoordinate heteroatom substituting the C–C bond and also the regioisomer number. For instance, the regioisomer [$C_{81}Pt_2$:**1**] is constructed after the substitution of the C5 atom by the first heteroatom and the substitution of the C2–C3 bond by the second heteroatom.

Table 7. Prediction by PLS analysis of the isomer stability of $C_{81}Pt_2$, a doped heterofullerene from isomer D_{2d} [C_{84}:**23**].[a]

Isomer number	Substituted C–C bonds[b]	Predicted relative energy[c]	Calculated relative energy	Pt–Pt[d]	no. C–C bonds	C–C bond length	no. heterorings
18	C20–C21	0.000	0.000	2.280	119	1.416	5
14	C3–C4	0.041		2.298	119	1.419	5
17	C19–C20	0.117		2.164	119	1.428	5
12	C1–C6	0.162		2.192	119	1.431	5
15	C4–C18	0.317		2.130	119	1.445	5
11	C6–C7	0.434		2.200	119	1.453	5
10	C7–C22	1.127	0.583	2.952	118	1.416	6
13	C1–C2	1.165		2.959	118	1.419	6
16	C18–C19	1.368		2.556	118	1.444	6
8	C42–C43	1.665		5.371	118	1.375	7
1	C2–C3	1.693		3.008	118	1.461	6
9	C21–C22	1.771	1.935	2.975	118	1.468	6
3	C32–C53	2.254		7.653	118	1.375	7
6	C79–C80	2.629		8.731	118	1.377	7
2	C13–C14	2.667	2.250	5.401	118	1.456	7
7	C63–C64	3.305		7.304	118	1.468	7
4	C71–C72	3.554	2.473	8.839	118	1.456	7
5	C82–C83	3.670		9.051	118	1.461	7

[a] The first platinum atom replaces the most pyramidalized carbon atom (C5, $\theta_p = 10.98°$) and thus it is tricoordinate. The second platinum atom substitutes a C_2 unit and is consequently the tetracoordinate one. Hence the $C_{81}Pt_2$ heterofullerene shares the same topology as $C_{57}Pt_2$. [b] The substituted C–C bond. See Figure 8 for the numbering system of D_{2d} [C_{84}:**23**]. [c] Predicted by using the PLS regression model for the four topological factors of $C_{57}Pt_2$. [d] Non-optimized Pt–Pt separation. The tricoordinate platinum atom is located 0.80 Å above the fullerene surface as platinum is in $C_{59}Pt$, whereas the tetracoordinate platinum atom is in the middle of the substituted C–C bond.

of D_{2d}-(C_{84}:**23**) are tabulated in Table S4 in the Supporting Information. Eighteen hypothetical regioisomers of $C_{81}Pt_2$ were built in which the tricoordinate heteroatom substitutes the most pyramidalized carbon atom (C5, $\theta_p = 10.98°$). The second heteroatom substitutes all C–C bonds through the C5–C6 symmetry plane, regioisomers [$C_{81}Pt_2$:**1--9**], and all the C–C bonds which would result in Pt–Pt separations of less than 3 Å, regioisomers [$C_{81}Pt_2$:**10--18**] (see Table 7 and Figure 8).

The values of the four factors used in the prediction are shown in Table 7. Since the geometries of the regioisomers of $C_{81}Pt_2$ were not optimized, the Pt–Pt separation was estimated from the free C_{60} and C_{84} structures: the tricoordinate heteroatom was placed 0.8 Å above the fullerene surface (like in $C_{59}Pt$) and the tetracoordinate heteroatom in the middle of the substituted C–C bond. Also, for C_{84}, the substituted C–C bond lengths were used instead of the type of C–C bond as a result of the higher variability in the bond lengths of this higher fullerene compared with C_{60}. Because of the different range of values of the factors for $C_{57}Pt_2$ and $C_{81}Pt_2$ we could not use the previously calculated regression model. Hence, a PLS model was calculated again by using the data for $C_{57}Pt_2$ with different preprocessing.[53]

The predicted relative energies are listed in Table 7. Their reliability was tested by comparing the predictions for representative regioisomers [$C_{81}Pt_2$:**2**, **4**, **9**, **10** and **18**] with the relative energies calculated from the fully optimized DFT geometries. Reliable relative energies were predicted by PLS analysis except for [$C_{81}Pt_2$:**4**] which has a longer Pt–Pt separation and is an extrapolation of the $C_{57}Pt_2$ PLS model. The mean difference between the calculated and predicted values for the first three calculated regioisomers was 0.375 eV, which is close to the prediction error expected for this model (0.283 eV), so we can consider the PLS predictions to be a good indication of the trends in the relative energies to be expected for regioisomers of $C_{81}Pt_2$. All the predictions are consistent with the knowledge acquired about the $C_{56}Pt_2$ and $C_{57}Pt_2$ heterofullerenes. Regioisomers [$C_{81}Pt_2$:**18, 14, 17, 12, 15**, and **11**] appear to be the most stable regioisomers of $C_{81}Pt_2$ because of short Pt–Pt distances, high numbers of retained C–C bonds and fewer heterorings in their structures. As for $C_{57}Pt_2$ the most stable substitutions are those that least distort the carbon framework of the D_{2d}–(C_{84}:**23**) fullerene. It is quite probable that the isomer [$C_{81}Pt_2$:**18**] is not the most stable of all the possible structures with formula $C_{81}Pt_2$ but this analysis shows that the present computational approach, DFT combined with PLS, is a powerful tool that may help in the study of multiple substitutions in a carbon cage.

Conclusions

When two platinum atoms replace two C_2 units, or one C_2 unit and one carbon atom in C_{60}, a priori, multiple isomers are possible. DFT calculations carried out on a high number of regioisomers of $C_{57}Pt_2$ and $C_{56}Pt_2$ clearly show that in the most stable structures the metal atoms occupy neighboring positions. Metal substitution produces deformation of the carbon framework and partial destruction of the fullerene aromaticity. This is the key factor determining the stability of these disubstituted clusters. Indeed, it is much easier to make a big hole that permits the incorporation of two platinum atoms in the carbon cage than two smaller holes on opposite hemispheres of the fullerene. The structures that have two neighbouring platinum atoms retain the greatest number of C–C bonds; this aspect is another important factor determining the stability of the cluster. In addition, clusters with short Pt–Pt contacts may contain weak metal–metal interactions, which also increase the stability of the cluster but are not a fundamental element of stability. This behavior is clearly different from that found in exohedral

metallofullerenes such as $[(\eta^2\text{-}C_{60})\{Pt(PH_3)_2\}_2]$ in which the double-metal addition occurs at opposite ends of the fullerene.[54]

In our opinion, the significance of these results extends beyond the particular cases of the $C_{57}Pt_2$ and $C_{56}Pt_2$ regioisomers; we believe that the conclusions drawn from this work can be extended to any transition-metal heterofullerene derivative. Calculations performed on the ionic species of the platinum derivatives and on some titanium homologues confirm the hypothesis that disubstituted C_{60} fullerenes should contain heteroatoms at adjacent sites. For larger fullerenes such as C_{70}, the behavior should be similar although in this case the curvature of the fullerene could also be important, as previously shown in monosubstituted species. Partial least-squares (PLS) regression analysis was used to analyse the interdependencies of all the factors that govern the stability of these clusters. We conclude that no factor by itself is capable of explaining the relative stabilities of the regioisomers but the combination of topological factors such as Pt–Pt separation, the number of C–C bonds, the type of C–C bond substitution and the number of heterorings are sufficient to identify satisfactorily the general trends of relative stability. Although curvature and an increase in the size of the cage can affect isomer stability, we have been able to predict the trends in the relative energies of the regioisomers of $C_{81}Pt_2$, a doped fullerene derived from the free D_{2d}-(C_{84}:**23**) fullerene, through a PLS regression model calculated by using the data for the analogous $C_{57}Pt_2$.

Acknowledgements

We thank the MCYT of the Government of Spain and the CIRIT of the Catalan Government (Grants n° BQU2002-04110-C02 02 and SGR01-00315) and the U.S. NSF (Grant 04 to A.L.B) for financial support.

[1] a) *The Chemistry of Fullerenes* (Ed.: R. Taylor), Advanced Series in Fullerenes, *Vol. 4*, World Scientific Publishing Co., Singapore, **1995**, p. 220; b) A. Hirsch, *The Chemistry of Fullerenes*, Thieme, Stuttgart, **1994**; c) *Fullerene Handbook* (Eds.: R. Ruoff, K. M. Kadish), Willey, New York, **1999**; d) A. L. Balch, M. M. Olmstead, *Chem. Rev.* **1998**, *98*, 2123.

[2] a) U. Reuter, A. Hirsch, *Carbon* **2000**, *38*, 1539; b) M. Keshavarzk, R. Gonzalez, R. G. Hicks, G. Srdanov, V. I. Srdanov, T. G. Collins, J. C. Hummelen, C. Bellavia-Lund, J. Pavlovich, F. Wudl, K. Holczer, *Nature* **1996**, *383*, 147; c) J. C. Hummelen, B. Knight, J. Pavlovich, R. Gonzalez, F. Wudl, *Science* **1995**, *269*, 1554; d) K. C. Kim, F. Hauke, A. Hirsch, P. D. W. Boyd, E. Carter, R. S. Armstrong, P. A. Lay, C. A. Reed, *J. Am. Chem. Soc.* **2003**, *125*, 4024.

[3] a) T. Guo, C. Jin, R. E. Smalley, *J. Phys. Chem.* **1991**, *95*, 4948; b) Y. Chai, T. Guo, C. Jin, R. E. Haufler, L. P. F. Chibante, J. Fure, L. Wang, J. M. Alford, R. E. Smalley, *J. Phys. Chem.* **1991**, *95*, 7564.

[4] T. Ohtsuki, K. Ohno, K. Shina, Y. Kawazoe, Y. Maruyama, K. Masumoto, *Phys. Rev. B* **1999**, *60*, 1531.

[5] C. Möschel, M. Z. Jansen, *Z. Anorg. Allg. Chem.* **1999**, *625*, 175.

[6] a) C. Bellavia-Lund, F. Wudl, *J. Am. Chem. Soc.* **1997**, *119*, 943; b) T. Pradeep, V. Vijayakrishnan, A. K. Santra, C. N. R. Rao, *J. Phys. Chem.* **1991**, *95*, 10564.

[7] a) B. Cao, X. Zhou, Z. Shi, Z. Jin, Z. Gu, H. Xiao, J. Wang, *Acta Phys.-Chim. Sin.* **1997**, *13*, 204; b) H. J. Muhr, R. Nesper, B. Schnyder, R. Kotz, *Chem. Phys. Lett.* **1996**, *249*, 399.

[8] H. Jiao, Z. Chen, A. Hirsch, W. Thiel, *J. Mol. Catal. B* **2003**, *9*, 34.

[9] a) W. Branz, I. M. L. Billas, N. Malinowski, F. Tast, M. Heinebrodt, T. P. Martin, *J. Chem. Phys.* **1998**, *109*, 3425; b) I. M. L. Billas, W. Branz, N. Malinowski, F. Tast, M. Heinebrodt, T. P. Martin, C. Massobrio, M. Boero, M. Parrinello, *Nanostruct. Mater.* **1999**, *12*, 1071.

[10] A. L. Balch, D. A. Costa, K. Winkler, *J. Am. Chem. Soc.* **1998**, *120*, 9614.

[11] A. Hayashi, Y. Xie, J. M. Poblet, J. M. Campanera, C. L. Lebrilla, A. L. Balch, *J. Phys. Chem. A* **2004**, *108*, 2192.

[12] a) A. Hirsch, B. Nuber, *Acc. Chem. Res.* **1999**, *32*, 795; b) Z. Chen, K. Ma, L. Chen, H. Zhao, Y. Pan, X. Zhao, A. Tang, J. Feng, *J. Mol. Struct.* **1998**, *452*, 219; c) Z. Chen, X. Zhao, A. Tang, *J. Phys. Chem. A* **1999**, *103*, 10961.

[13] Z. Chen, U. Reuther, A. Hirsch, W. Thiel, *J. Phys. Chem. A* **2001**, *105*, 8105.

[14] H. Jiao, Z. Chen, A. Hirsch, W. Thiel, *Phys. Chem. Chem. Phys.* **2002**, *4*, 4916.

[15] L. Turker, *J. Mol. Struct.* **2002**, *593*, 149.

[16] I. M. L. Billas, C. Massobrio, M. Boero, M. Parrinello, W. Branz, F. Tast, N. Malinowski, M. Heinebrodt, T. P. Martin, *J. Chem. Phys.* **1999**, *111*, 6787.

[17] J. M. Poblet, J. Muñoz, K. Winkler, M. Cancilla, A. Hayashi, C. B. Lebrilla, A. L. Balch, *Chem. Commun.* **1999**, 493.

[18] C. G. Ding, J. L. Yang, X. Y. Cui, C. T. Chan, *J. Chem. Phys.* **1999**, *110*, 8481.

[19] C. G. Ding, J. L. Yang, R. Han, K. Wang, *Phys. Rev. A* **2001**, *64*, 43201.

[20] a) ADF 2000.01, Department of Theoretical Chemistry, Vrije Universiteit, Amsterdam (www.scm.com); b) E. J. Baerends, D. E. Ellis, P. Ros, *Chem. Phys.* **1973**, *2*, 41; c) L. Versluis, T. Ziegler, *J. Chem. Phys.* **1988**, *88*, 322; d) G. te Velde, E. J. Baerends, *J. Comput. Phys.* **1992**, *99*, 84; e) C. F. Guerra, J. G. Snijders, G. te Velde, E. J. Baerends, *Theor. Chem. Acc.* **1998**, *99*, 391.

[21] S. H. Vosko, L. Wilk, M. Nusair, *Can. J. Phys.* **1980**, *58*, 1200.

[22] a) A. D. Becke, *J. Chem. Phys.* **1986**, *84*, 4524; b) A. D. Becke, *Phys. Rev.* **1988**, A38, 3098.

[23] a) J. P. Perdew, *Phys. Rev.* **1986**, *84*, 4524; b) J. P. Perdew, *Phys. Rev. A* **1986**, *34*, 7406.

[24] a) J. G. Snijders, E. J. Baerends, P. Vernooijs, *At. Nucl. Data Tables* **1982**, *26*, 483; b) P. Vernooijs, J. G. Snijders, E. J. Baerends, *Slater type basis functions for the whole periodic system*, Internal Report, Free University of Amsterdam, The Netherlands, **1981**.

[25] Xaim, J. C. Ortiz, C. Bo, Universitat Rovira i Virgili, Tarragona (Spain), **1999**. Xaim is freely available at www.quimica.urv.es/XAIM

[26] a) P. Geladi, B. R. Kowalski, *Anal. Chim. Acta* **1986**, *185*, 1; b) H. Martens, T. Naes, *Multivariate Calibration*, Wiley, New York, **1989**; c) Unscrambler 8.0, Camo As., Trondheim (Norway).

[27] W. H. Powell, F. Cozzi, G. P. Moss, C. Thilgen, R. J.-R. Hwu, A. Yerin, *Pure Appl. Chem.* **2002**, *74*, 629.

[28] E. J. Baerends, V. Branchadell, M. Sodupe, *Chem. Phys. Lett.* **1997**, *265*, 481.

[29] D. L. Lichtenberger, K. W. Nebesny, C. D. Ray, D. R. Huffman, L. D. Lamb, *Chem. Phys. Lett.* **1991**, *176*, 203.

[30] S. H. Yang, C. L. Pettiette, J. Concienciao, O. Cheshnowsky, R. E. Smalley, *Chem. Phys. Lett.* **1991**, *139*, 233.

[31] F. H. Allen, *Acta Crystallogr. Sect. B* **2002**, *58*, 380.

[32] N. W. Alcock, P. Bergamini, T. M. Gomes-Carniero, R. D. Jackson, J. Nicholls, A. G. Orpen, P. G. Pringle, S. Sostero, O. Traverso, *J. Chem. Soc., Chem. Commun.* **1990**, *4*, 980.

[33] a) R. W. F. Bader, *Atoms in Molecules, A Quantum Theory*, Clarendon Press, Oxford, **1990**; b) R. W. F. Bader, P. J. MacDougall, C. D. H. Lau, *J. Am. Chem. Soc.* **1984**, *106*, 1594.

[34] According to the theory of Atoms in Molecules, the presence of a (3,–1) bond critical point (bcp) linking two atoms is sufficient for the presence of a bond.

[35] M. Bénard, M. M. Rohmer, J. M. Poblet, *Chem. Soc. Rev.* **2000**, *29*, 495.
[36] a) N. Kurita, K. Kobayashi, H. Kumabora, K. Tago, *Phys. Rev. B* **1993**, *48*, 4850; b) N. Kurita, K. Kobayashi, H. Kumabora, K. Tago, K. Ozawa, *Chem. Phys. Lett.* **1992**, *198*, 95; c) N. Kurita, K. Kobayashi, H. Kumabora, K. Tago, *Fullerene Sci. Technol.* **1993**, *1*, 319.
[37] Z. Chen, K. Ma, Y. Pan, X. Zhao, A. Tang, J. Feng, *J. Chem. Soc. Faraday Trans.* **1998**, *94*, 2269.
[38] When two metal atoms are close together, only one hole is necessary in the dimetallic heterofullerenes and this situation is energetically more favorable than the double perforation of the carbon skeleton that occurs when, for example, the two metal atoms are in different hemispheres.
[39] Not all regioisomers have the same number of C–C and Pt–C bonds. Structures with metal–metal contacts have more C–C bonds, although there are correspondingly fewer Pt–C bonds. We have checked that it is preferable to maintain the number of C–C before creating Pt–C bonds.
[40] Previous calculations on the monosubstituted $C_{58}Pt$ and $C_{58}Ir$ heterofullerenes have shown that substitution of a [6:5] C–C bond by a metal instead of a [6:6] C–C bond is less favorable by 0.58 eV for platinum and by 0.61 eV for Ir, see ref. [11].
[41] The number of rings that contain a heteroatom gives an indirect measure of the change in the carbon skeleton and it is closely related to the metal–metal distance.
[42] Cage radius is defined as the average distance between all the surface atoms and the center of the fullerene.
[43] a) J. Kruszewski, T. M. Krygowski, *Tetrahedron Lett.* **1972**, *13*, 3839; b) T. M. Krygowski, *J. Chem. Inf. Comput. Sci.* **1993**, *33*, 70.
[44] T. M. Krygowski, M. K. Cyranski, *Chem. Rev.* **2001**, *101*, 1385.
[45] The change in aromaticity could also be a measure of the distortion of the carbon skeleton of the fullerene. The HOMA index is a geometric measure of aromaticity. HOMA varies from 0 for nonaromatic systems to 1 for fully aromatic systems. The values of HOMA calculated at the present level of computation for the reference systems of benzene, C_{60}, $C_{59}Pt$, $C_{58}Pt$:66 and $C_{58}Pt$:65 were computed to be 0.969, 0.274, 0.268, 0.279 and 0.240, respectively. Another aromatic index that could be used is the NICS (nucleus independent chemical shift), which is based on magnetic criteria. This index has not been used in this study.
[46] D. L. Massart, B. G. M. Vandeginste, L. M. C. Buydens, S. De Jong, P. J. Lewi, J. Smeyers-Verbeke, *Handbook of Chemometrics and Qualimetrics*, Elsevier Science, Amsterdam, **1998**, Parts A and B.
[47] The variable C–C bond type was coded as 1 and 0, corresponding to [6:6] and [6:5], respectively. All the *x* variables were then autoscaled so that each variable had the same a priori importance in the calculation of the model.
[48] Data were handled as in the PLS analysis of Table 4 except that, in this case, the variable C–C bond type was coded as 0, 1 and 2. The biplot is shown in Figure S2 in the Supporting Information.
[49] a) P. W. Fowler, D. E. Manolopoulos, *An Atlas of Fullerenes*, Oxford, **1995**; b) B. L. Zhang, C. Z. Wang, K. M. Ho, *J. Chem. Phys.* **1992**, *96*, 7183; c) X. Q. Wang, C. Z. Wang, B. L. Zhang, K. M. Ho, *Phys. Rev. Lett.* **1992**, *69*, 69; d) X. Q. Wang, C. Z. Wang, B. L. Zhang, K. M. Ho, *Chem. Phys. Lett.* **1993**, *207*, 349.
[50] The numbering system of D_{2d} (C_{84}:**23**) was extracted from R. Taylor, *J. Chem. Soc., Perkin Trans. 2* **1993**, 813.
[51] a) R. C. Haddon, L. T. Scott, *Pure Appl. Chem.* **1986**, *58*, 137; b) R. C. Haddon, *J. Am. Chem. Soc.* **1986**, *108*, 2837; c) R. C. Haddon, S. Y. Chow, *J. Am. Chem. Soc.* **1998**, *120*, 10494.
[52] The pyramidalisation angle of carbon atoms (θ_p), which is a measure of fullerene sphericity, was not been taken into account in the analysis of C_{60} because all the carbon atoms have the same value however it could also be important. According to Ding et al. (ref. [18]) it has an important effect on the regioisomers of $C_{69}M$, a doped fullerene of C_{70}, in which M replaces the most pyramidalized carbon atom.
[53] The four topological factors of $C_{57}Pt_2$ were range-scaled between 0 and 1. The data in Table 7 were scaled so that a variation in the scaled variables of $C_{57}Pt_2$ and Table 7 corresponded to the same variation in the original *x* variables. The RMSEP of the new PLS model was 0.283 eV, which is similar to the value obtained for the autoscaled data, hence the different scaling did not reduce the predictive performance of the model. In this case the PLS model represents 84% of the original four topological *x* variables and 90% of the relative energy of $C_{57}Pt_2$. The plot of DFT-calculated relative energies versus PLS-predicted relative energies for this PLS model is shown in Figure S3 in the Supporting Information.
[54] a) P. J. Fagan, J. C. Calabrese, B. Malone, *J. Am. Chem. Soc.* **1991**, *113*, 9408; b) P. J. Fagan, J. C. Calabrese, B. Malone, *Acc. Chem. Res.* **1992**, *25*, 134; c) A. L. Balch, J. W. Lee, B. C. Noll, M. M. Olmstead, *J. Am. Chem. Soc.* **1992**, *114*, 10984; d) C. Bo, M. Costas, J. M. Poblet, *J. Phys. Chem.* **1995**, *99*, 5914.

Received: August 9, 2004
Revised: December 3, 2004
Published online: February 25, 2005